Scope of the C–S Insertion Reaction of Thiazolium Salts with Platinum(0) Diphosphine Complexes

Virginia C. M. Smith,† Robin T. Aplin,† John M. Brown,*,† Michael B. Hursthouse,‡ Alexander I. Karalulov,‡ K. M. Abdul Malik,‡ and Neil A. Cooley§

Contribution from Dyson Perrins Laboratory, South Parks Road, Oxford OX1 3QY, U.K., Department of Chemistry, University of Wales, P.O. Box 912, Cardiff CF1 3TB, Wales, and BP Chemicals Research Laboratory, Sunbury-on-Thames, Middlesex TW16 7LN, U.K.

Received June 28, 1993. Revised Manuscript Received November 18, 1993®

Abstract: When 3-methylthiazolium iodide or BF_4^- is reacted with 1,1′-bis(diphenylphosphino)ferrocene-η^2-ethene-platinum (**10**) above –40 °C, a rapid displacement reaction occurs, leading to the formation of a ring-expanded adduct **11** by formal C–S insertion; a 2:1 adduct **12** is formed sequentially. Thiazole, its *N*-oxide, and oxazole do not show this type of reactivity under these conditions, although a related 1:1 adduct is formed by thiazole·HO_3SCF_3, and both 1:1 and 2:1 adducts from the benzothiazole·BF_3 complex. With 2,3-dimethylthiazolium BF_4^-, the reaction is much slower and the product **14** arises from a C–S insertion reaction of opposite regiochemistry. With 3-methylbenzothiazolium BF_4^-, a similar sequence occurs, and the 1:1 adduct **17** and the 2:1 adduct **18** have been characterized crystallographically. In the benzothiazolium series, the 2,3-dimethyl derivative behaves similarly to the parent, giving product **19**. Similar chemistry was observed initially with 2-chloro-3-methylbenzothiazolium BF_4^- on reaction with **10**, but rearrangement occurs subsequently to give the C–Cl insertion product **21**. C–S cleavage of *S*,*N*,*N*-trimethylthioformamidinium BF_4^- is observed on reaction with **10**, giving the C–S insertion product **22**. Electrospray MS played an important role in determining the solution structures of several of the Pt complexes described.

Introduction

Activation and cleavage of the C–S bond in condensed thiophenes is a critical component of catalytic hydrodesulfurization during the refining of crude oils. Although the typical commercial catalyst composition is cobalt/molybdenum sulfide supported on alumina,[1] many other metals and combinations are active. The reactivity of low-valent transition-metal complexes toward thiophenes has provided important information on the possible modes of thiophene coordination and the accessibility of ring-opening routes.[2]

The diversity of structural chemistry is illustrated by recent examples. Thermolysis of arylrhodium hydride **1** in the presence of a slight excess of thiophene gave rise to the formal C–S insertion product **2**. Analogous results were obtained with 2,5-dimethylthiophene or benzothiophene, for which C2–S is the preferred site of metal insertion. With dibenzothiophene, a second, less stable product is also formed by C–H insertion of the metal.[3] Photolysis of dihydride **3** in the presence of thiophene at –40 °C led to the formation of complex **2** together with the metastable C–H insertion product **4**, which reverted to it (via S-η^1 or η^2 transient intermediates) at ambient temperature.[4] Reaction of $Cp^*Rh(C_2H_4)_2$ with thiophene at 90 °C gave the dimeric ring-opened product **5**.[5] When the ethene displacement was carried out photochemically, a transient monomeric intermediate postulated to be **6a** was observed. With 2-methoxythiophene, metallathiabenzene **6b** was characterized in solution in equilibrium with Rh=S [2 + 2] cyclodimers.[5]

Other low-valent transition-metal complexes are reactive toward the C–S bond of thiophenes. The η^4-arene iridium complex **7** was the first product of reduction of the corresponding dicationic bis(tetrafluoroborate) with Red-Al, but rearranged to the C–S insertion product **8** in the presence of base or when in contact with basic alumina. For complex **8**, as for the Rh analogs **6**, an aromatic iridathiabenzene structure was postulated.[6] The reaction of $Cp^*Co(C_2H_4)_2$ with excess thiophene at 70 °C gave a bridged dicobalt complex **9** in 80% yield;[7] the ^1H NMR spectrum indicated fluxionality involving transposition of the coordinated and free double bonds. Similar bimetallic bridged thiophenes had been observed or postulated previously, first as Fe and then later as Rh complexes.[8]

Alongside studies of the organometallic chemistry of thiophene encouraged by HDS, there is parallel literature on the metal complexation of thiazoles and related heterocycles, motivated by their biological interest.[9] The most common mode of thiazole coordination is η^1-N, although sulfur complexation in this and related series has been observed. Pd and particularly Pt are most frequently employed, and the chemistry of coordinated thiazoles differs from that of thiophenes in that metal insertion into the C–S bond has not previously been observed.

† Dyson Perrins Laboratory.
‡ University of Wales.
§ BP Chemical Research Laboratory.
® Abstract published in *Advance ACS Abstracts,* April 1, 1994.

(1) Curtis, M. D. *Appl. Organomet. Chem.* **1992**, *6*, 429. Startsev, A. N. *Usp. Khim.* **1992**, *61*, 332.
(2) Reviews: Angelici, R. J. *Acc. Chem. Res.* **1988**, *21*, 387. Reynolds, J. G. *Chem. Ind.* **1991**, 570. Luh, T. Y.; Ni, Z. J. *Synthesis* **1990**, 89. Rauchfuss, T. B. *Prog. Inorg. Chem.* **1991**, *39*, 259. Wiegand, B. C.; Friend, C. M. *Chem. Rev.* **1992**, *92*, 491. Angelici, R. J. *Coord. Chem. Rev.* **1990**, *105*, 61.
(3) Jones, W. D.; Dong, L. Z. *J. Am. Chem. Soc.* **1991**, *113*, 559. Cf.: Selnau, H. E.; Merola, J. S. *Organometallics* **1993**, *12*, 1583.
(4) Dong, L. Z.; Duckett, S. B.; Ohman, K. F.; Jones, W. D. *J. Am. Chem. Soc.* **1992**, *114*, 151.
(5) Jones, W. D.; Chin, R. M. *J. Am. Chem. Soc.* **1992**, *114*, 9851.
(6) Chen, J. B.; Daniels, L. M.; Angelici, R. J. *J. Am. Chem. Soc.* **1991**, *113*, 2544. Chen, J.; Angelici, R. J. *Organometallics* **1990**, *9*, 849. Chen, J. B.; Daniels, L. M.; Angelici, R. J. *J. Am. Chem. Soc.* **1990**, *112*, 199.
(7) Jones, W. D.; Chin, R. M. *Organometallics* **1992**, *11*, 2698.
(8) Hubener, P.; Weiss, E. *J. Organomet. Chem.* **1977**, *129*, 105–115. Luo, S. F.; Skaugset, A. E.; Rauchfuss, T. B.; Wilson, S. R. *J. Am. Chem. Soc.* **1992**, *114*, 1732.
(9) Muir, M. M.; Cox, O.; Rivera, L. A.; Cadiz, M. E.; Medina, E. *Inorg. Chim. Acta* **1992**, *191*, 131–9. Van Beusichem, M.; Farrell, N. *Inorg. Chem.* **1992**, *31*, 634–9. Rong, M.; Muir, M. M.; Cadiz, M. E.; Muir, J. A. *Acta Crystallogr. C* **1991**, *47*, 1539–41. Muir, M. M.; Gomez, G. M.; Cadiz, M. E.; Muir, J. A. *Inorg. Chim. Acta* **1990**, *168*, 47–57. Muir, M. M.; Cadiz, M. E.; Baez, A. *Inorg. Chim. Acta* **1988**, *151*, 209–213.

0002-7863/94/1516-5180$04.50/0

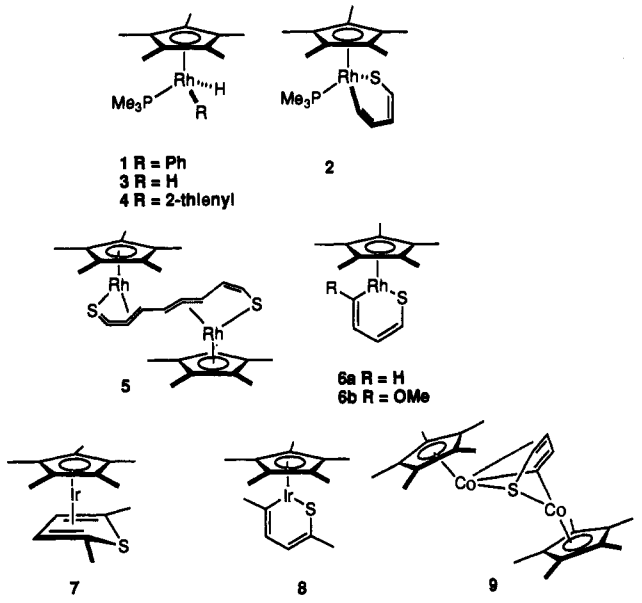

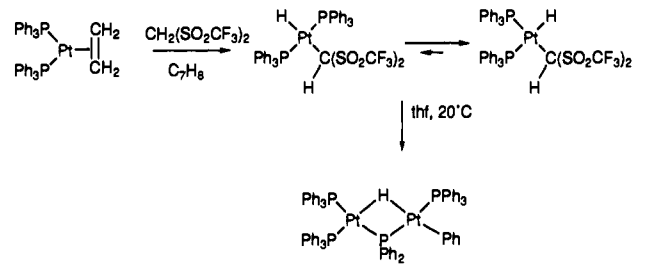

Figure 1. Heterolytic C–H activation of a disulfone by bis(triphenylphosphine)Pt(C_2H_4).[10]

Results and Discussion

During a project intended to develop the catalytic organometallic chemistry of C–H acids, we examined the reactivity of various species with Pt(0) complexes, with the precedent of Figure 1 in mind.[10] The chelating diphosphine complex 1,1′-bis(diphenylphosphino)ferrocene-η^2-etheneplatinum (**10**), prepared as previously described for $P_2Pt(C_2H_4)$ analogs,[11] was employed because of its stability, favorable solubility characteristics, and reactivity toward ethene displacement. Reactions can readily be followed by ^{31}P NMR; the Pt ethene complex **10** appears as a singlet at δ 29 ppm, J_{PtP} = 3683 Hz; Pt–P and P–P couplings give important information on both the structure and the electronic character of any displacement product. Although the experiments did not lead to C–H activation novel C–S insertion chemistry was observed, related to the thiophene chemistry described in the Introduction.

Thiazolium Salts. Simple 3-methylthiazolium salts possess a pK_a (H_2O) of around 16.5 for ionization of H2, permitting the possibility of C–H activation by an ionic mechanism.[12] The experimental protocol involved mixing of the reactant with Pt ethene complex **10** in CH_2Cl_2 solution and monitoring the ^{31}P NMR spectrum, when it was observed that 3-methylthiazolium iodide was very rapidly solubilized. The resulting spectrum indicated two new species in unequal amounts, with the exact proportions depending on precise reaction conditions. The course was similar in MeOH/CH_2Cl_2 (1:1), and where both components were in solution, reaction occurred rapidly at or below –50 °C. Neither thiazole nor thiophene showed any reactivity under these conditions, and oxazolium salts reacted very slowly to give a variety of products. The reaction of 3-methylthiazolium BF_4^- was examined in more detail (Table 1). It was established that the reaction occurred in two stages, the second requiring a further mole of Pt ethene complex **10** to react with the initially formed species. The rate of reaction was limited only by the rate of dissolution of the thiazolium salt. By ^{31}P NMR spectral analysis of the reaction as it proceeded, it was estimated that formation of the first product was half-complete after 30 min at –44 °C; the second product only appeared in the late stages of reaction. Crystallization from CH_2Cl_2/petroleum permitted the isolation of the first compound, established by analysis to be a 1:1 adduct. The ^{31}P NMR was consistent with a C, S-bound species (J_{PPt} = 3023, 2109 Hz),[13] and this together with several features of the ^1H NMR spectrum indicated the formation of a C–S insertion product. Of the two alternatives for the insertion product (dppf)Pt(C_4H_6NS)$^+BF_4^-$, regioisomeric form **11** was suggested by the unique low-field proton in the ^1H NMR spectrum at 9.00 ppm, which gave an NOE enhancement of 9.5% in *ortho*-PPh_2 protons and 11% in the *N*-Me protons at 3.55 ppm. This low-field proton, H6, has a 20-Hz coupling to Pt, and selective heteronuclear decoupling established couplings of 9 and 22 Hz to P *trans* to C and P *trans* to S, respectively. The proton at 7.07 ppm must be H4 because of the strong (11%) NOE to the N–Me group and ^3J and ^4J proton couplings of 7.5 and 1.7 Hz, respectively, but it has no P or Pt couplings. The remaining vinyl proton in the metallocyclic ring, H3, is obscured by the aryl protons of the ligand, but revealed to resonate at 7.60 ppm by 2-D COSY analysis, which indicated its direct coupling to H4. The compound is stable in solution and in the solid state and showed no sign of reverting to the thiazolium salt. Under conditions where the parent thiazolium salt rapidly exchanged ^2H (MeOD, iPr_2NEt), platinacycle **11** remained unchanged, indicating that the characteristic C–H acidity of thiazolium salts is lost after Pt insertion.

When a further equivalent of the Pt ethene complex **10** was added to a solution of insertion product **11** in CH_2Cl_2 at ambient temperature, complete conversion into a new species, identical to the one formed in small quantities during the initial experiments, was observed. A 2:1 stoichiometry was confirmed by NMR and mass spectra and analysis. The ^{31}P NMR spectrum is second-order, and the P–Pt coupling *trans* to S is much greater than in complex **11**; the spectrum can be simulated only if long-range P–Pt couplings are included (Table 1). The ^1H NMR spectrum, assigned with the help of NOE, COSY, and heteronuclear decoupling as before, indicates gross differences in chemical shift compared to the monomeric complex; H6 is now at 4.41 ppm and possesses a 27-Hz coupling to both platinum nuclei, but no discernible P coupling. Proton H4 resonates at 6.65 ppm, and H3 at 3.95 ppm, with broadening due to the two Pt couplings; the *N*-methyl group is also at much higher field, 1.71 ppm. A gross structure for [(dppf)$_2$Pt$_2$(C_4H_6NS)]$^+BF_4^-$ akin to **12** was suggested on this basis, but detailed analysis deferred because of clarification through work on the benzothiazole analog (*vide infra*).

The related diphosphine Pt(C_2H_4) complexes **13a** and **13b** were examined (Table 1) and behaved in a broadly similar way, save that more of the 2:1 complexes than before was produced in CH_2Cl_2. The C_2 symmetry of the ligand requires that the pairs of phosphorus nuclei *trans* to S or to C are diastereotopic in the 2:1

(10) Siedle, A. R.; Newmark, R. A.; Gleason, W. B. *J. Am. Chem. Soc.* **1986**, *108*, 767–73.

(11) Brown, J. M.; Cook, S. J.; Kimber, S. J. *J. Organomet. Chem.* **1984**, *269*, C58. Brown, J. M.; Cooley, N. A.; Price, D. W. *J. Chem. Soc., Chem. Commun.* **1989**, 458–60. Parker, D.; Taylor, R. J. *J. Chem. Soc., Chem. Commun.* **1987**, 1781–2. Cf.: Nagel, U. *Chem. Ber.* **1982**, *115*, 1998.

(12) Bordwell, F. G.; Satish, A. V. *J. Am. Chem. Soc.* **1991**, *113*, 985–90. Chen, Y.-T.; Jordan, F. *J. Org. Chem.* **1991**, *56*, 5029–38 and references therein. Elvidge, J. A.; Jones, J. R.; O'Brien, C.; Evans, E. A.; Sheppard, H. C. *Adv. Heterocyclic Chem.* **1974**, *16*, 1–30.

(13) Cf.: Cairns, M. A.; Dixon, K. R.; Rivett, G. A. *J. Organomet. Chem.* **1979**, *171*, 373–385.

(14) Bleke, J. A.; Xie, Y.-F.; Peng, W.-J.; Chiang, M. *J. Am. Chem. Soc.* **1989**, *111*, 4118.

Table 1. Reactions of Thiazolium Species with Pt Ethene Complex **10** (Unless Otherwise Stated)

entry	reactant (1 equiv)	conditions	product ratio (%) 1:1 complex	2:1 complex	16[f]	^{31}P NMR data for 1:1 complexes δ_P	J_{PP}	J_{PPt}	^{31}P NMR data for 2:1 complexes δ_P	J_{PP}	J_{PPt}
1	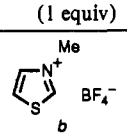	CH_2Cl_2/rt/1 h	88[a]	12[a]		25.3	27	3023	16.7	14	4219
2	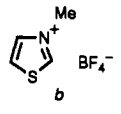	CH_2Cl_2:MeOH (1:1)/ rt/1 h	100	0		18.5	2109	12.7			2255/60
3[c]	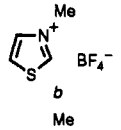	CH_2Cl_2/rt/1 h	24[e]	76		7.8 –0.2	28	2837 1970	5.4 2.0 1.1 –5.3	br br 	4107 2215/62 4140 2191/67
4[d]	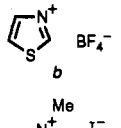	CH_2Cl_2/rt/1 h	60	40		13.5 4.7	27	2865 1986	12.6 9.8 6.0 –0.7	6 6 	4049 2190/54 4211 2182/62
5	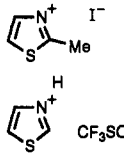	CH_2Cl_2/rt/24 h	100[a]	0		22.4 19.9	26	3476 2042			
6	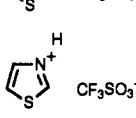	$CDCl_3$/rt/15 min	77[e]	8	15[e]	22.8	27	3035	17.6	13	4262
7	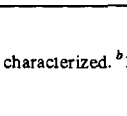	CH_2Cl_2:MeOH (1:1)/ rt/1 h	31	0	69	20.7		2051	13.0		2303/57

[a] Fully characterized. [b] 1.1 equiv employed. [c] 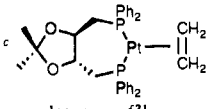 13a employed. [d] 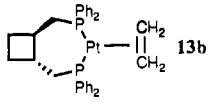 13b employed.

[e] Product identification by mass spectrometry and ^{1}H NMR. [f] ^{31}P NMR data for **16** δp: 27.0 (J_{PP} = 15 Hz, J_{PPt} = 1730 Hz, P *trans* to C), 13.5 (J_{PPt} = 4304 Hz, P *trans* to N).

complexes; in keeping with this, four broadened but distinct ^{31}P resonances are observed.

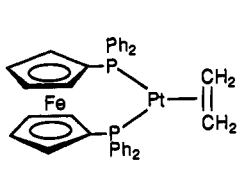

10

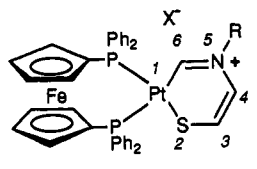

11 R = Me
15 R = H

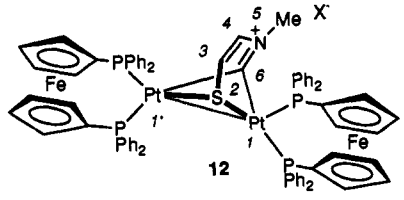

12

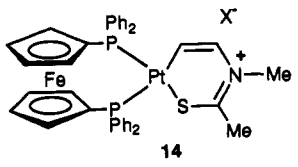

14

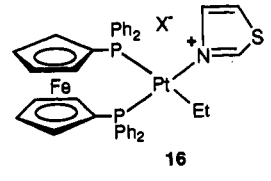

16

The reaction of Pt ethene complex **10** with 2,3-dimethylthiazolium iodide in CH_2Cl_2 was much slower and gave a single product, which was isolated in 78% yield and fully characterized (Table 1, entry 5). The ^{31}P spectrum of the product (Figure 2A), and particularly J_{PPt} values, indicated some structural similarity to 1:1 complex **11**, but the ^{1}H NMR spectrum revealed clear differences between them. The two vinylic hydrogens H5 and H6 at 6.76 and 6.70 are both strongly coupled to Pt and one of the two phosphorus nuclei (J_{HPt} = 64 and 23 Hz, respectively); the C–CH_3 group at 2.52 ppm possesses a 12-Hz coupling to Pt. This demonstrates that this 1:1 product (dppf)Pt(C_5H_8NS)$^+$I$^-$ (**14**) is formed by an insertion process regioisomeric with that leading to the parent compound **11**, a conclusion reinforced by the fact that the C–Me group at 2.5 ppm has rather weak NOEs to several aromatic protons, rather than the strong *ortho*-contacts which would be expected for its regioisomer. The selectivity for this process seems to be complete, since ^{31}P NMR spectral peaks which could correspond to the alternative isomer were not observed on monitoring. Neither thiazole nor thiophene reacted with the Pt ethene complex **10** under ambient conditions. The parent thiazolium–NH triflate was comparable in its reactivity toward complex **10** to the 3-methylthiazolium salt, producing mainly the analogous 1:1 C–S insertion product (dppf)Pt(C_3H_4NS)$^+$$CF_3SO_3^-$ (**15**) together with a small quantity of a probable 2:1 complex, characterised by P–Pt couplings of 2303 and 4262 Hz. A third compound was apparent, and under the conditions of Table 1, entry 7 this was the major component. The ^{1}H NMR and electrospray MS of this compound indicated the presence of a Pt-bound ethyl (dppf)Pt(C_3H_3NS)C_2H_5, as in structure **16**. Its formation indicates that the thiazolium salt acts as a proton source toward the coordinated ethene and traps the intermediate formed by coordination of the N-lone pair of thiazole. Interconversion between the complexes **16** and **15** was not observed, and hence they are probably formed on separate pathways. When the C–S

Table 2. Reactions of Benzothiazolium Species with Pt Ethene Complex **10**

entry	reactant (1 equiv)	conditions	product ratio (%) 1:1 complex	product ratio (%) 2:1 complex	^{31}P NMR data for 1:1 complexes δ_P	^{31}P NMR data for 1:1 complexes J_{PP}	^{31}P NMR data for 1:1 complexes J_{PPt}	^{31}P NMR data for 2:1 complexes δ_P	^{31}P NMR data for 2:1 complexes J_{PP}	^{31}P NMR data for 2:1 complexes J_{PPt}
1	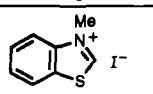	CH_2Cl_2/rt/1 h	38[a]	62[a]	21.9	22	3096	17.6	14	4329
2	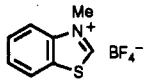	CH_2Cl_2:MeOH (1:1)/ rt/15 min	80[b]	20[b]	14.7		2262	14.6		2029/59
3	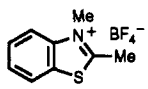	CH_2Cl_2/rt/15 min	100[b]	0	18.4 11.1	20	3298 2212			
4	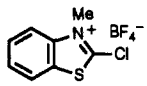	CD_2Cl_2/rt/15 min	81[b,c]	0	19.4 10.3	20	3222 2542			
5	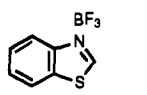	CH_2Cl_2/rt/15 min	64	36	22.5 18.5	25	3049 2125	18.5 14.9	14	4394 2145/58

[a] Trace diiodide also observed. [b] Fully characterized. [c] Rearranged product **21** (19%).

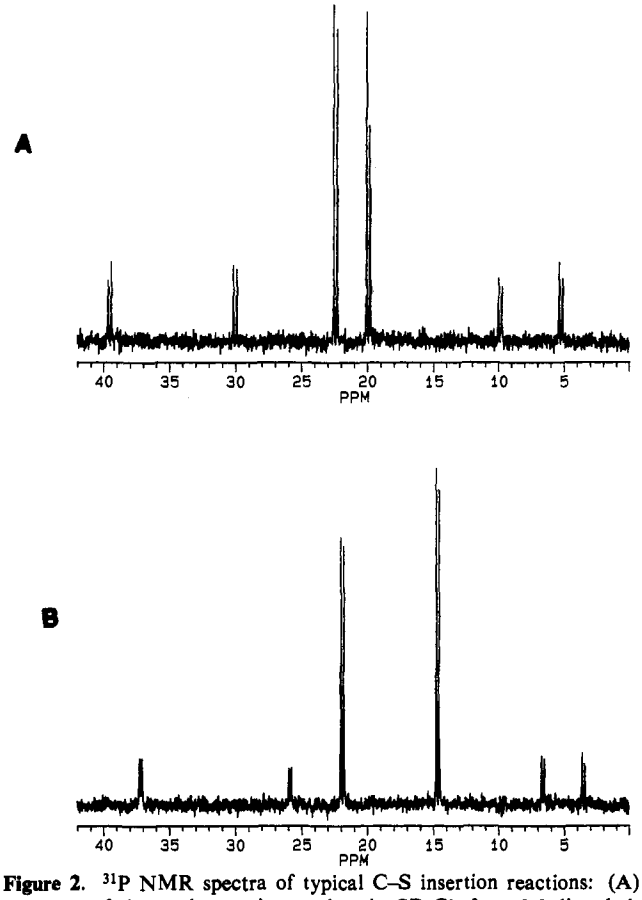

Figure 2. ^{31}P NMR spectra of typical C–S insertion reactions: (A) spectrum of the crude reaction product in CD_2Cl_2 from 2,3-dimethylthiazolium iodide and complex **10** (Table 1, entry 5); (B) spectrum of isolated and purified complex **17** (X = BF_4^-) in CD_2Cl_2 (cf. Table 2, entry 1).

insertion product **15** was treated with NEt_3, decomposition occurred and some thiazole was observed in the ^{1}H NMR, implying that the neutral species formed by N-deprotonation of complex **15** is unstable with respect to reversion to the uncomplexed heterocycle.

Benzothiazolium Salts. The experiments described in Table 1 demonstrate the extreme facility of insertion of Pt(0) into the C–S bond of thiazolium salts, and it was of interest to extend the generality of this observation. The reactions of 3-methylbenzothiazolium iodide with Pt ethene complex **10** are described in

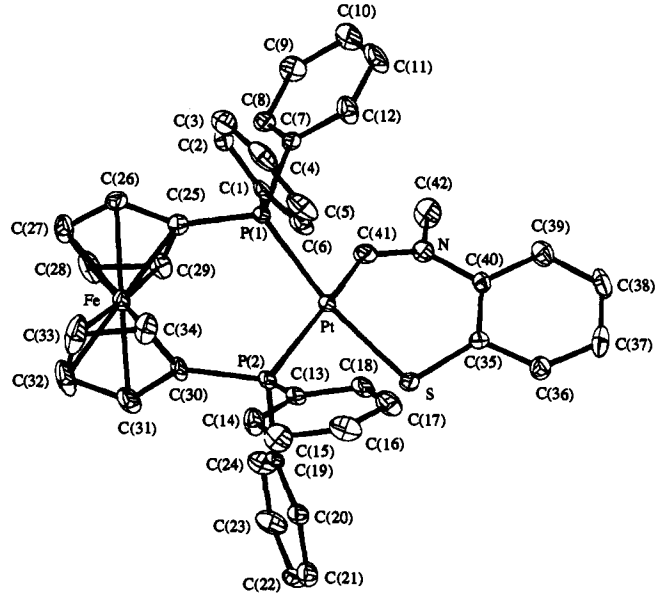

Figure 3. ORTEP plot of the X-ray crystal structure of the cationic fragment of complex **17** ($C_{42}H_{36}FeNP_2PtSBF_4$), with hydrogen atoms removed for clarity. Principal bond lengths and angles are shown in Table 3. Crystallographic numbering conventions are followed here and in Table 3.

Table 2 and follow a similar course, albeit with easier formation of the 2:1 complex. Separate conditions were developed which favored the isolation of X-ray quality crystals of both the 1:1 complex and the 2:1 complex. The first was solved and refined to a final *R*-value of 0.032; the resulting structure of complex (dppf)Pt(C_8H_8NS)$^+BF_4^-$ (**17**) is shown in Figure 3; selected bond lengths and angles are summarized in Table 3. The essential features of the metallocycle derived by C2–S insertion confirm the earlier NMR analyses and in addition define the conformation of the metallocyclic ring. Inspection reveals that the N–C4–C3–S unit is nearly coplanar, as is the Pt–C6–N–C4 unit, with those planes mutually twisted (Figure 4A). The N–C6 bond length of 1.283 Å is significantly shorter than that in typical thiazolium salts,[15] indicating that its double-bond character is high, despite the out-of-plane distortion. This core structure can be compared with two metallocyclic complexes derived from thiophene, which are also displayed in Figure 4. The coordi-

(15) Aoki, K. *Acta Crystallogr. B* **1988**, *45*, 1926. Dupont, L. *Acta Crystallogr. C* **1989**, *45*, 1926.

Table 3. Selected Bond Lengths (Å) and Angles (deg) for **17**

Pt–C(41)	2.006(5)	Pt–P(1)	2.292(2)
Pt–P(2)	2.355(1)	Pt–S	2.306(2)
S–C(35)	1.753(6)	N–C(40)	1.435(7)
N–C(41)	1.283(7)	N–C(42)	1.507(7)
C(35)–C(40)	1.409(8)		
C(41)–Pt–P(1)	88.5(2)	C(41)–Pt–S	88.0(2)
P(1)–Pt–S	170.4(1)	C(41)–Pt–P(2)	162.1(2)
P(1)–Pt–P(2)	96.8(1)	S–Pt–P(2)	89.2(1)
C(35)–S–Pt	106.5(2)	N–C(41)–Pt	134.9(5)
C(41)–N–C(40)	125.6(5)	C(41)–N–C(42)	117.5(5)
C(40)–N–C(42)	116.9(5)	C(40)–C(35)–S	127.3(4)
C(36)–C(35)–S	116.1(4)	C(35)–C(40)–N	121.1(5)

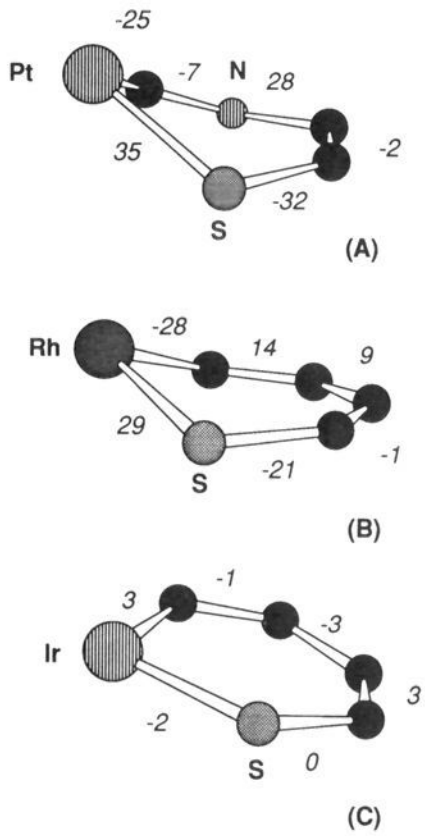

Figure 4. Comparison of the X-ray-derived metallocycle geometry in three M–S six-ring unsaturated heterocycles: (A) monomer **17**, taken from this work and showing the boat-like conformation about the light heteroatoms; italicized numbers refer to the torsion angles about the endocyclic bonds; (B) 2,4-dimethylthiophene-derived analog of coordinatively saturated complex **2**, with the Rh atom out of the plane described by the other atoms; (C) coordinatively unsaturated metallobenzene core of complex **8**.

natively saturated rhodium complex **6** depicted in Figure 4B also posseses a nonplanar ring, with the rhodium displaced out of the plane describing the five light atoms. In contrast, iridium complex **8** shown in Figure 4C possesses a near-planar six-membered ring, consistent with its formulation as an iridathiabenzene complex[14] with C3–S significantly shortened relative to the standard single-bond length and the C–C bond lengths within the diene fragment all comparable.

The ^{1}H NMR spectrum of benzothiazolium insertion product **17** displays several features in common with the analog **11** discussed above. There is a distinctive low-field proton H6 at 8.66 ppm with phosphorus couplings of 11.7 and 6.4 Hz, and with broad satellites due to a Pt coupling of about 19 Hz. The *N*-methyl group at 3.56 ppm displays strong NOEs to H6 and to an *ortho*-proton at 7.45 ppm. Since the ^{31}P NMR spectra of the two 1:1 insertion products **17** and **11** are rather similar, it is inferred that they are isostructural. The general similarities within this series of compounds is revealed by the spectrum of complex **17** displayed in Figure 2B.

The X-ray structure of the 2:1 monocationic complex $[(dppf)_2Pt_2(C_8H_8NS)]^+BF_4^-$ (**18**) was also solved, when the data were refined as a racemic twin. The resulting structure of the cationic portion of the dimer is shown in Figure 5, and selected bond lengths and angles are presented in Table 4. This study reveals the symmetrical nature of the thiazolium bridge between

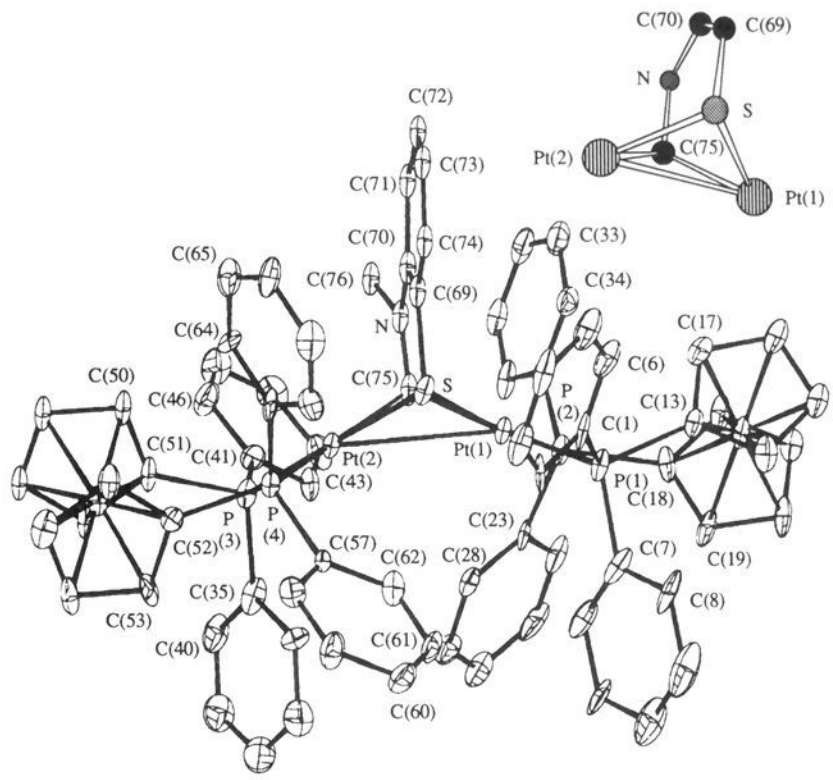

Figure 5. ORTEP plot of the X-ray crystal structure of the cationic fragment of complex **18** ($C_{76}H_{64}Fe_2NP_4Pt_2SBF_4$). The Pt_2 core is inset. Principal bond lengths and angles are shown in Table 4. Crystallographic numbering conventions are followed here and in Table 4.

Table 4. Selected Bond Lengths (Å) and Angles (deg) for **18**

Pt(1)–Pt(2)	3.069(2)	S(1)–C(69)	1.80(2)
S(1)–Pt(1)	2.339(6)	S(1)–Pt(2)	2.339(6)
Pt(1)–P(1)	2.342(6)	Pt(2)–P(3)	2.286(6)
Pt(1)–P(2)	2.279(5)	Pt(2)–P(4)	2.341(6)
Pt(1)–C(75)	2.13(2)	Pt(2)–C(75)	2.20(2)
C(69)–C(70)	1.41(3)	C(70)–N(1)	1.40(2)
C(75)–N(1)	1.30(3)	C(76)–N(1)	1.57(3)
C(75)–Pt(1)–P(2)	87.6(6)	C(75)–Pt(1)–S(1)	77.5(6)
P(2)–Pt(1)–S(1)	164.4(2)	C(75)–Pt(1)–P(1)	170.2(6)
P(2)–Pt(1)–P(1)	101.8(2)	S(1)–Pt(1)–P(1)	92.9(6)
C(75)–Pt(2)–S(1)	76.1(5)	C(75)–Pt(2)–P(3)	96.8(6)
P(3)–Pt(2)–S(1)	173.0(2)	C(75)–Pt(2)–P(4)	162.5(6)
P(3)–Pt(2)–P(4)	100.5(2)	S(1)–Pt(2)–P(4)	86.5(2)
C(69)–S(1)–Pt(1)	101.2(7)	C(69)–S(1)–Pt(2)	104.2(7)
Pt(1)–S(1)–Pt(2)	82.0(2)	C(74)–C(69)–C(70)	123(2)
C(74)–C(69)–S(1)	117(2)	C(70)–C(69)–S(1)	120(2)
N(1)–C(70)–C(69)	124(2)	N(1)–C(70)–C(71)	117(2)
N(1)–C(75)–Pt(1)	116(2)	N(1)–C(75)–Pt(2)	112(2)
C(75)–N(1)–C(70)	127(2)	C(75)–N(1)–C(76)	118(2)
C(70)–N(1)–C(76)	115(2)	Pt(1)–C(75)–Pt(2)	90.2(9)

the two Pt atoms. The C5–S bond has been cleaved, and its terminii form the bridge without participation of the other ring atoms; the five atoms of the original heteroaromatic ring are essentially coplanar. There is probably weak Pt–Pt bonding at the observed distance of 3.069(2) Å, reinforced by the observation of second-order splittings due to Pt–Pt coupling in the ^{31}P NMR spectrum, although these are less clear-cut than in the case of the simple 2:1 thiazolium complex **12**. The bonding is different from that observed in the crystallographically characterized dicobalt complex **9** or in an iron species described earlier, in which the bridging ligand is unsymmetrically bonded to the two metal atoms.[7,8]

In the ^{1}H NMR spectrum of benzothiazolium 2:1 complex **18**, the isolated C–H of the expanded thiazolium ring is at 4.6 ppm and its pseudotriplet appearance can be simulated by H–Pt_2 coupling of 26 Hz. As in dimer **18**, the *N*-methyl group is strongly shielded relative to the monomer and resonates at 1.6 ppm.

The BF_3 adduct of benzothiazole reacted rapidly with Pt ethene complex **10** in CH_2Cl_2, again giving a mixture of the 1:1 and 2:1 products, as judged by the characteristic ^{31}P NMR spectra. With 2,3-dimethylbenzothiazolium BF_4^-, however, only a single 1:1 complex was produced, in 98% isolated yield after 15 min, and

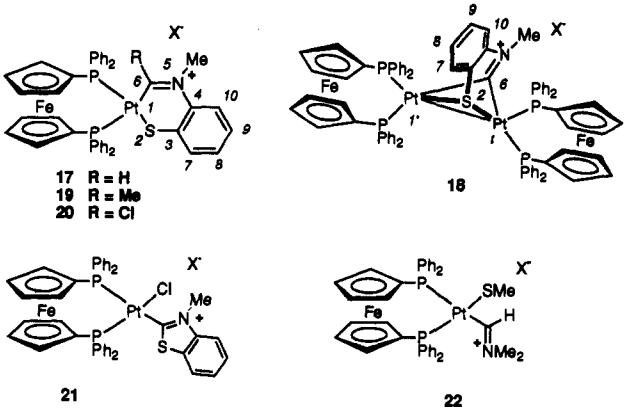

the ^{1}H NMR spectrum makes it evident that this product, (dppf)Pt($C_9H_{10}NS$)$^+BF_4^-$ (**19**), is formed by insertion between the S and C2 atoms and not adjacent to the arene; in the ^{1}H NMR spectrum, there is a Pt–H coupling of 23 Hz as well as an H–P coupling of 3 Hz to the *C*-methyl group at 2.1 ppm; the *N*-methyl group is at 3.4 ppm. Yet different behavior is observed for 2-chloro-3-methylbenzothiazolium BF_4^- salt. In CH_2Cl_2 or THF, the reaction with Pt ethene complex **10** went to completion within a few minutes at ambient temperature, giving mainly the C–S insertion 1:1 adduct (dppf)Pt(C_8H_7ClNS)$^+BF_4^-$ (**20**) (J_{PPt} = 3223, 2543 Hz; δ N-Me = 3.60 ppm), following the precedent described. This can be isolated if workup is carried out immediately, but if the solution is kept and monitored over several days, then gradual rearrangement to a new chloroplatinum complex occurs (this being present as a minor component in the initial reaction product), in which the thiazolium ring has reformed. This rearrangement product has NMR spectra indicative of the structure (dppf)Pt(C_8H_7NS)Cl$^+BF_4^-$ (**21**), e.g. J_{PPt} = 3682, 2390 Hz. This latter class of compound, but not the intermediate, had previously been observed by Stone and co-workers[16] in their studies of the organometallic chemistry of 2-halothiazoles as potential carbene precursors. The sequence of reactions indicates that the endocyclic S–C bond is kinetically more labile to Pt(0) than the exocyclic Pt–Cl bond.

Since all of the reactions described involve the insertion of Pt into an activated C–S bond adjacent to an immonium ion, it was of interest to see whether this type of reaction was shown by the parent *S,N,N*-trimethylthioformamidinium BF_4^-. Accordingly, the salt was reacted with Pt ethene complex **10** in THF, leading to the now familiar change in the ^{31}P NMR spectrum to a Pt-coupled AB quartet corresponding to the C–S insertion product. An analytically pure and stable sample of the complex (dppf)Pt($C_4H_{10}NS$)$^+BF_4^-$ (**22**) was isolated and the ^{1}H NMR spectrum delineated. The distinct low-field proton at 9.96 ppm in $CDCl_3$ (10.32 ppm in $(CD_3)_2CO$) exhibits ^{31}P couplings of 4 and 6 Hz and a ^{195}Pt coupling of 20 Hz. By means of selective NOE experiments, the (*Z*) N-Me at 3.60 ppm and the (*E*) N-Me at 2.95 ppm were located; the S-Me resonance is then at 2.1 ppm. Interestingly, the latter possesses a 50-Hz coupling to Pt, not apparent for the sp^2 hybridized 2H in the platinacyclic analog **11**. The NOEs of 4–6% observed between the (*Z*) N-Me and diverse aromatic protons indicate that the metalloamidine residue is not held rigidly in the square plane and can move into van der Waals contact with the diphosphine ligand.

Electrospray MS of Platinum Complexes. There have already been several successful applications of the electrospray MS technique[17] to organometallic chemistry.[18] It was found that well-defined parent–cation spectra were generally obtained when

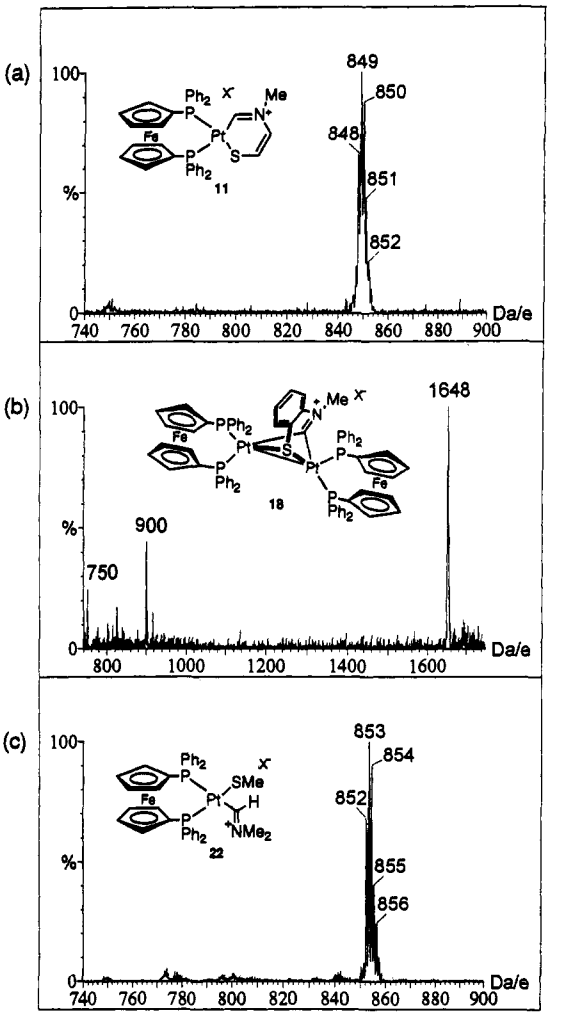

Figure 6. Typical electrospray MS recorded as described in the supplementary material: (a) monomeric complex **11**; (b) 2:1 complex **18**; (c) complex **22**.

the cationic complexes described herein were subjected to electrospray MS. This is in contrast to their typical behavior under FAB MS conditions, since there are severe problems arising from ligand exchange with the matrix (e.g. dithiothreitol, dithioerythritol, or *meta*-nitrobenzyl alcohol) or decomposition, and the parent peak is often not the dominant fragment. Generally speaking, the insertion products from C–S activation give very clean spectra (see the examples in Figure 6), and the calculated isotope ratio is in accord with observation, leading in these cases to unequivocal identification of the cationic fragment. In all cases examined the parent peak predominated.

Mechanism of the Thiazolium Insertion Reactions. A satisfactory mechanism for the C–S insertion chemistry needs to explain the regiochemistry and the high reactivity of thiazolium salts relative to other heterocycles. The S-basicity of thiophene is much lower than that of a dialkyl sulfide,[19] and that of thiazolium

(16) Fraser, J. P.; Roper, W. R.; Stone, F. G. A. *J. Chem. Soc., Dalton Trans.* **1974**, 102.

(17) Fenn, J. B.; Mann, M.; Meng, C. K.; Wong, S. F.; Whitehouse, C. M. *Science* **1989**, *246*, 64.

(18) Ashton, P. R.; Brown, C. L.; Chapman, J. R.; Gallagher, R. T.; Stoddart, J. F. *Tetrahedron Lett.* **1992**, *33*, 7771. Curtis, J. M.; Derrick, P. J.; Schnell, A.; Constantin, E.; Gallagher, R. T.; Chapman, J. R. *Inorg. Chim. Acta* **1992**, *201*, 197. Curtis, J. M.; Derrick, P. J.; Schnell, A.; Constantin, E.; Gallagher, R. T.; Chapman, J. R. *Org. Mass Spectrom.* **1992**, *27*, 1176. Colton, R.; Traeger, J. C. *Inorg. Chim. Acta* **1992**, *201*, 153. Colton, R.; Tedesco, V.; Traeger, J. C. *Inorg. Chem.* **1992**, *31*, 3865. Poon, G. K.; Mistry, P.; Lewis, S. *Biol. Mass Spectrom.* **1991**, *20*, 687. Henry, K. D.; Quinn, J. P.; McLafferty, F. W. *J. Am. Chem. Soc.* **1991**, *113*, 5447.

(19) The gas-phase proton affinity of thiophene is >6 kcal mol^{-1} less than that of dimethyl sulfide, but the difference is in fact much greater because the S-protonation of thiophene is strongly disfavored with respect to α-protonation: Houriet, R.; Schwarz, H.; Zummack, W.; Andrade, J. G.; Schleyer, P. v. R. *Nouv. J. Chim.* **1981**, *5*, 505. Meot-Ner, M.; Sieck, L. W. *J. Am. Chem. Soc.* **1991**, *113*, 4448.

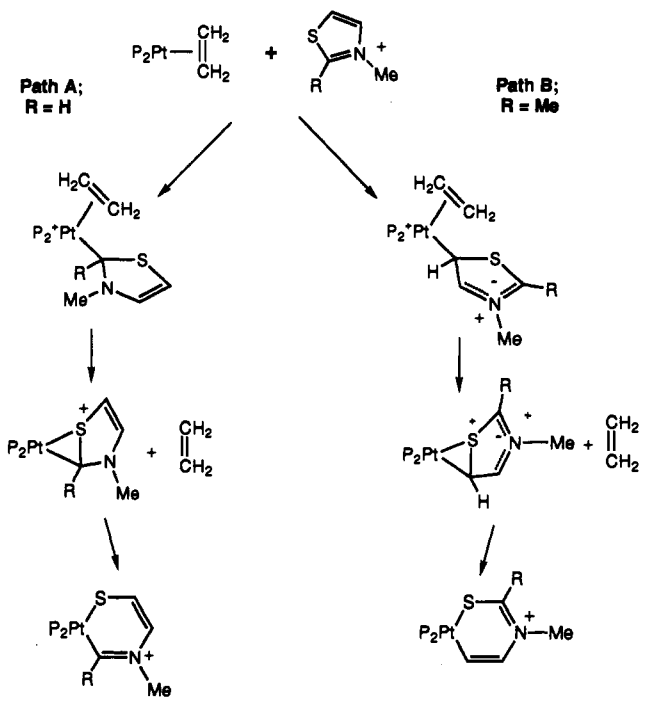

Figure 7. A mechanism for the ring-opening process, based on initial nucleophilic attack on C2 of the thiazolium ring. Steric repulsion by a methyl group at C2 redirects the attack to C5.

salts is likely to be lower still, which militates against initial η^1-coordination with the metal playing an electrophilic role. In alkene/alkene displacements at Pt(0), the metal entity is predominantly nucleophilic in character, reacting faster with electrophilic alkenes.[20] This in itself explains the relative reactivity of thiazolium ions and thiazoles. It is further known that the main site of nucleophilic attack in 3-alkylthiazolium cations is at C2 and that alkylation at C2 decreases the reactivity by a factor of 100-fold.[21] Nucleophilic attack at C5 is not observed in monocyclic systems, but the equivalent site is the target of morpholine addition in a fused tricyclic thiazolium cation.[22] These analogies provide a rationalization for the observed C–S insertion chemistry of thiazolium salts.

The reaction can then be envisaged as occurring by the route outlined in Figure 7. The initial reversible coordination of C2 to platinum is followed by loss of ethene with concurrent sulfur coordination, along path A. A simple bond reorganization leads to the observed C–S insertion product. Complex **14** formed by S–C5 insertion into the 2,3-dimethylthiazolium salt is produced by path B, avoiding the steric constraints of the normally preferred route. The first intermediate on this path can be represented (in one canonical form) as an azomethine ylid.[23] Again, the loss of ethene with sulfur coordination led to a further intermediate which rearranges to product. Path B, which requires initial nucleophilic attack at C5 of the thiazolium salt, is expected to be disfavored for benzothiazolium salts even when there is a substituent at C2, since that first step will disrupt aromatic conjugation.

In sterically unencumbered cases the 1:1 complexes are quite reactive toward a further molecule of the Pt ethene complex **10**. This second addition may occur by initial nucleophilic attack of Pt at the iminium carbon (C5), which will be very electrophilic in the adducts; product formation is completed by attack of sulfur on the cationic Pt center created. The bimetallic 2:1 product is formally a 6,7-dimetallabicyclo[3.1.1]heptane, for which analogies exist.[24]

Conclusions

Overall, the series of reactions described demonstrate the high reactivity toward metal-mediated cleavage of the C–S bond of the functional group RS–C=NR_2^+ in cyclic or open-chain systems, which has not previously been observed. Enhanced reactivity of the electrophilic iminium carbon is implicated in that attack. The work suggests a number of further experiments which will extend the basic observation to other metals and to related iminium ion derivatives. The metalloamidines so generated are rare in organometallic chemistry and are expected to possess interesting reactivity.

Experimental Section

General Methods. Elemental microanalyses were carried out by Mrs. V. Lamburn in the Dyson Perrins Laboratory, using a Carlo Erba 1106 elemental analyzer. ^{1}H NMR spectra were recorded on Bruker AM 250 (250 MHz) or Bruker AM 500 (500 MHz) spectrometers. COSY and NOE experiments were carried out by Mrs. E. McGuinness using a Bruker AM 500 (500 MHz) spectrometer; second-order spectra were simulated using the microprogram NMR" (Calleo Scientific). ^{31}P NMR spectra were recorded on a Bruker AM 250 (101.3 MHz) spectrometer and are referenced externally to 85% phosphoric acid. ^{1}H{^{31}P} NMR spectra were recorded on a Bruker AM 500 (500 MHz) spectrometer with a home-built heteronuclear decoupler trolley, using selective continuous wave phosphorus irradiation. These spectra were acquired on ^{1}H decoupler coils of a selective ^{31}P probe with the usual observation coil acting as the decoupler coil. IR spectra were recorded on a Perkin-Elmer 1750 FT spectrometer. Melting points were recorded on a Reichert–Köfler block and are uncorrected. All manipulations of oxygen- and water-sensitive materials were carried out under an argon atmosphere using standard vacuum line and Schlenk techniques. The compounds 1,1′-bis(diphenylphosphino)ferrocene-η^2-etheneplatinum (**10**),[25] (*R*,*R*)-[2,2-dimethyl-1,3-dioxolane-4,5-diyl)bis(methylene)]bis(diphenylphosphine)-η^2-etheneplatinum (**13a**),[11] 2-methylthiazole,[26] 3-methylthiazolium iodide,[27] 3-methylbenzothiazolium iodide,[28] 2,3-dimethylbenzothiazolium BF_4^-,[29] 2,3-dimethylthiazolium iodide,[30] and 2-chloro-3-methylbenzothiazolium BF_4^- [16] were prepared according to literature procedures. (*R*-(−)-1,2-Bis(diphenylphosphinomethyl)cyclobutane)-η^2-etheneplatinum (**13b**) was prepared by methods analogous to **10**,[11] mp >88 °C (dec); 3-methylthiazolium BF_4^-, 3-methylbenzothiazolium BF_4^-, and *S*,*N*,*N*-trimethylthioformamidinium BF_4^- were prepared by methylation of the parent compounds with trimethyloxonium tetrafluoroborate. Thiazolium triflate was prepared by protonation of thiazole with trifluoromethanesulfonic acid. Solvents were purchased from Rhone–Poulenc and were dried prior to use according to the procedures described by Perrin and Armarego.[31] Deuterated solvents and reagents were purchased from the Aldrich Chemical Co. or from Lancaster Chemicals.

^{31}P NMR Experiments: General Method. The thiazolium salt (1 equiv unless otherwise stated) was added, as a solid, to the bis(phosphine)-(η^2-ethene)Pt complex (0.03 mmol) dissolved in the desired solvent (2.4 mL), in an 8-mm NMR tube, under a stream of Ar (Tables 1 and 2). The suspension was vigorously agitated to aid dissolution, and in several cases the evolution of ethene was observed. ^{31}P NMR integration was used to determine product ratios.

(20) Parker, D.; Taylor, R. J. *Tetrahedron* **1988**, *44*, 2241.
(21) Bunting, J. W. *Adv. Heterocyclic Chem.* **1979**, *25*, 1–82
(22) Hajos, G.; Messmer, A.; Koritsansky, T. *J. Org. Chem.* **1987**, *52*, 2015–8.
(23) Lown, J. W. In *1,3-Dipolar Cycloaddition Chemistry*; Padwa, A., Ed.; Wiley-Interscience: New York, 1984; Vol. 1, Chapter 6, pp 653–732.
(24) *Inter alia*: Lin, W.; Wilson, S. R.; Girolami, G. S. *J. Chem. Soc., Chem. Commun.* **1993**, 284–5. Aumann, R.; Averbeck, H.; Kruger, C. *Chem. Ber.* **1975**, *108*, 3336–48. King, J. A., Jr.; Vollhardt, K. P. C. *J. Am. Chem. Soc.* **1983**, *105*, 4846–8.
(25) Analytically pure complex **10** was prepared by the method of ref 11. Brown, J. M.; Perez-Torrente, J. J. *Organometallics*, manuscript in preparation, 1993 carries the full description.
(26) Hantzsch, A. *Ann. Chem.* **1889**, *250*, 257.
(27) Hafferl, W.; Lundin, R.; Ingram, L. L. *Biochemistry* **1963**, *2*, 1298.
(28) Nigrey, P. J.; Garito, A. F. *J. Chem. Eng. Data* **1977**, *22*, 451.
(29) Reichardt, C.; Mormann, W. *Chem. Ber.* **1972**, *105*, 1815.
(30) Hojo, M.; Masuda, R.; Kosaka, S.; Nagase, K. *Synthesis* **1979**, 272.
(31) Perrin, D. D.; Armarego, W. L. F. *Purification of Laboratory Chemicals*, 3rd ed.; Pergamon Press: New York, 1988.

Synthesis of 11. 3-Methylthiazolium BF_4^- (10.3 mg, 0.055 mmol) was added to a solution of 1,1′-bis(diphenylphosphino)ferrocene-η^2-etheneplatinum (**10**) (38.9 mg, 0.05 mmol) in CH_2Cl_2 (1 mL) and MeOH (1 mL) and vigorously stirred for 5 min. Concentration *in vacuo* yielded an orange oil, which was dissolved in CH_2Cl_2 (1 mL) and, after filtration, was transferred via cannula into light petroleum (50 mL) to precipitate the product as a yellow solid (44 mg, 94%). Mp dec > 157 °C. Anal. Calcd for $C_{38}H_{34}BF_4FeNP_2PtS$: C, 48.74; H, 3.66; N, 1.50; S, 3.42. Found: C, 48.72; H, 3.95; N, 1.39; S, 3.17. ^{1}H NMR (500 MHz; $CDCl_3$): 9.00 (1H, dd, $J_{HP(trans\ S)}$ = 22.3 Hz, $J_{HP(trans\ C)}$ = 9.4 Hz, J_{HPt} = 20.0 Hz, H6), 7.68–7.59 (11H, m, 10 H Ph and H3), 7.54 (2H, t, $^3J_{HH}$ = 7.5 Hz, Ph), 7.49–7.41 (8H, m, Ph), 7.07 (1H, dd, J_{HH} = 8.0 Hz, J = 1.6 Hz, H4), 4.58 (2H, br s, Cp), 4.49 (2H, s, Cp*), 4.39 (2H, br s, Cp), 4.13 (2H, br s, Cp*), 3.51 (3H, s, N-Me). ^{31}P NMR (101.3 MHz; CH_2Cl_2:MeOH (1:1)): 25.3 (d, J_{PP} = 27 Hz, J_{PPt} = 3023 Hz, P *trans* to S), 18.5 (d, J_{PPt} = 2109 Hz, P *trans* to C). IR (KBr disc): 3054 (w), 2955 (w), 1631 (br, w), 1481 (w), 1436 (m), 1168 (s), 1055 (s, br), 749 (m), 697 (s), 553 (m), 517 (m), 494 (m), 470 (m) cm^{-1}.

Synthesis of 12. 1,1′-Bis(diphenylphosphino)ferrocene-η^2-etheneplatinum (**10**) (7.8 mg, 0.01 mmol) and **11** (9.4 mg, 0.01 mmol) were dissolved in CH_2Cl_2 (2 mL) in an 8-mm NMR tube, and the suspension was vigorously agitated. ^{31}P NMR showed complete conversion to **12** after 5 min. The yellow solution was transferred via cannula into light petroleum (40 mL) to precipitate the product as a yellow solid (15.6 mg, 92%). Mp dec > 198 °C. Anal. Calcd for $C_{72}H_{62}BF_4Fe_2NP_4Pt_2S$: C, 51.29; H, 3.71; N, 0.83. Found: C, 51.00; H, 3.58; N, 0.73. ^{1}H NMR (500 MHz; $CDCl_3$): 7.94 (4H, dd, $J_{HP(trans\ S)}$ = 11.3 Hz, $^3J_{HH}$ = 7.6 Hz, *o*-H Ph *trans* S), 7.88 (4H, dd, $J_{HP(trans\ C)}$ = 10.7 Hz, $^3J_{HH}$ = 8.0 Hz, *o*-H Ph *trans* C), 7.56 (2H, t, $^3J_{HH}$ = 7.5 Hz, *p*-H Ph *trans* S), 7.51 (2H, t, $^3J_{HH}$ = 7.5 Hz, *p*-H Ph *trans* C), 7.33 (2H, t, $^3J_{HH}$ = 7.4 Hz, *p*-H Ph), 7.26 (2H, t, $^3J_{HH}$ = 7.3 Hz, *p*-H Ph), 7.21–7.12 (16H, m, *m*-H Ph), 6.99–6.95 (8H, m, *o*-H Ph), 6.65 (1H, br d, J_{HH} = 6.3 Hz, H4), 4.41 (1H, t, J_{HPt} = 26.6 Hz, H6), 4.30 (2H, br s, Cp), 4.28 (2H, br s, Cp*), 4.20 (2H, br s, Cp), 4.16 (2H, br s, Cp*), 3.97 (2H, br s, Cp), 3.95 (1H, m, H3), 3.93 (2H, br s, Cp*), 3.84 (2H, br s, Cp), 3.80 (2H, br s, Cp*), 1.71 (3H, s, N-Me). ^{31}P NMR (101.3 MHz; CH_2Cl_2): 16.7 (2P, d, J_{PP} = 14 Hz, J_{PPt} = 4219 Hz, P *trans* to S), 12.7 (2P, d, J_{PPt} = 2255 Hz, J_{PPt} = 60 Hz, P *trans* to C). IR (KBr disc): 3052 (w), 1587 (w), 1481 (m), 1436 (s), 1166 (m), 1097 (s), 1084 (s), 1054 (s, br), 748 (m), 696 (s), 544 (m), 516 (m), 493 (m), 469 (m) cm^{-1}.

Synthesis of 14. 2,3-Dimethylthiazolium iodide (14.5 mg, 0.06 mmol) was added to a solution of 1,1′-bis(diphenylphosphino)ferrocene-η^2-etheneplatinum (**10**) (46.6 mg, 0.06 mmol) in CH_2Cl_2 (3 mL) and was stirred for 24 h. The orange solution was transferred via cannula into light petroleum (40 mL) to precipitate the product as an orange solid (46 mg, 78%). Mp dec > 186 °C. Anal. Calcd for $C_{39}H_{36}FeINP_2PtS$: C, 47.27; H, 3.66; N, 1.41; S, 3.24. Found: C, 47.03; H, 3.60; N, 1.37; S, 2.87. ^{1}H NMR (500 MHz; CD_2Cl_2): 7.73 (4H, dd, $J_{HP(trans\ S)}$ = 11.8 Hz, J_{HH} = 8.2 Hz, *o*-H Ph *trans* S), 7.60–7.56 (6H, m, Ph), 7.53–7.48 (6H, m, Ph), 7.38 (4H, td, $^3J_{HH}$ = 7.8 Hz, J = 2.3 Hz, *m*-H Ph), 6.76 (1H, ddd, $J_{HP(trans\ C)}$ = 15.0 Hz, J_{HH} = 9.5 Hz, $J_{HP(trans\ S)}$ = 1.1 Hz, J_{HPt} = 64.0 Hz, H5), 6.70 (1H, ddd, $J_{HP(trans\ S)}$ = 23.9 Hz, $J_{HP(trans\ C)}$ = 5.1 Hz, J_{HPt} = 22.8 Hz, H6), 4.57 (2H, br s, Cp), 4.56 (2H, br s, Cp), 4.36 (2H, br s, Cp), 3.80 (2H, br s, Cp), 3.74 (3H, s, N-Me), 2.52 (3H, s, J_{HPt} = 12.2 Hz, C-Me). ^{31}P NMR (101.3 MHz; CD_2Cl_2): 22.4 (d, J_{PP} = 26 Hz, J_{PPt} = 3476 Hz, P *trans* to S), 19.9 (d, J_{PPt} = 2042 Hz, P *trans* to C). IR (KBr disc): 3045 (w), 1587 (w), 1480 (m), 1435 (s), 1167 (m), 1097 (s), 1028 (m), 748 (s), 697 (s), 637 (w), 552 (s), 516 (s), 494 (s), 470 (s) cm^{-1}.

Synthesis of 17 and 18. 3-Methylbenzothiazolium BF_4^- (11.9 mg, 0.05 mmol) was added to a solution of 1,1′-bis(diphenylphosphino)-ferrocene-η^2-etheneplatinum (**10**) (38.9 mg, 0.05 mmol) in CH_2Cl_2 (1.2 mL) and MeOH (1.2 mL) in an 8-mm NMR tube and the suspension vigorously agitated. The immediate formation of the main product, **17**, was observed by ^{31}P NMR. After concentration *in vacuo* to ca. 1.5 mL the side product **18** precipitated from the yellow solution as orange crystals (3 days) (10 mg, 23%). Mp dec > 152 °C. Anal. Calcd for $C_{76}H_{64}BF_4Fe_2NP_4Pt_2S$: C, 52.58; H, 3.72; N, 0.81; S, 1.85. Found: C, 52.64; H, 3.77; N, 0.56; S, 1.80. ^{1}H NMR (500 MHz; $CDCl_3$): 8.01 (4H, dd, $J_{HP(trans\ S)}$ = 11.7 Hz, $^3J_{HH}$ = 7.5 Hz, *o*-H Ph^1 *trans* S), 7.95 (4H, dd, $J_{HP(trans\ C)}$ = 10.7 Hz, $^3J_{HH}$= 7.1 Hz, *o*-H Ph^2 *trans* C), 7.60 (2H, t, $^3J_{HH}$ = 8.6 Hz, *p*-H Ph^1 *trans* S), 7.59 (2H, t, $^3J_{HH}$ = 8.2 Hz, *p*-H Ph^2 *trans* C), 7.34 (2H, t, $^3J_{HH}$ = 7.4 Hz, *p*-H Ph^3 *trans* S), 7.28 (2H, td, $^3J_{HH}$ = 7.4 Hz, $^4J_{HH}$ = 1.0 Hz, *p*-H Ph^4 *trans* C), 7.19–7.22 (5H, m, *m*-H Ph^2 *trans* C and H9), 7.10–7.17 (12H, m, *m*-H Ph^1 Ph^3 Ph^4), 6.93 (4H, dd, $J_{HP(trans\ S)}$ = 11.0 Hz, $^3J_{HH}$ = 7.6 Hz, *o*-H Ph^3 *trans* S), 6.87 (4H, dd, $J_{HP(trans\ C)}$ = 9.9 Hz, $^3J_{HH}$ = 7.7 Hz, *o*-H Ph^4 *trans* C), 6.71 (1H, d, J_{HH} = 8.5 Hz, H10), 6.62 (1H, t, J_{HH} = 7.3 Hz, H8), 6.36 (1H, dd, $^3J_{HH}$ = 7.8 Hz, $^4J_{HH}$ = 1.5 Hz, H7), 4.58 (1H, t, J_{HPt} = 26.0 Hz, H6), 4.26 (2H, br s, Cp), 4.23 (2H, s, Cp*), 4.17 (2H, s, Cp), 4.13 (2H, s, Cp*), 3.87 (2H, br s, Cp), 3.84 (2H, s, Cp*), 3.81 (2H, s, Cp), 3.78 (2H, m, Cp*), 1.60 (3H, s, N-Me). ^{31}P NMR (101.3 MHz; CH_2Cl_2): 17.7 (2P, d, J_{PP} = 14 Hz, J_{PPt} = 4329 Hz, P *trans* to S), 14.6 (2P, d, J_{PPt} = 2029 Hz, J_{PPt} = 59 Hz, P *trans* to C). IR (KBr disc): 3051 (w), 1586 (w), 1483 (s), 1436 (s), 1308 (w), 1166 (m), 1098 (s), 1052 (s, br), 1037 (s), 746 (s), 696 (s), 547 (m), 515 (m), 492 (s), 468 (s) cm^{-1}. The mother liquor was transferred via cannula into light petroleum (50 mL) to precipitate the product **17** as a yellow solid (31 mg, 63%). Mp dec > 160 °C. Anal. Calcd for $C_{42}H_{36}BF_4FeNP_2PtS$: C, 51.13; H, 3.68; N, 1.42; S, 3.25. Found: C, 51.40; H, 3.92; N, 1.47; S, 2.98. ^{1}H NMR (500 MHz; CD_2Cl_2): 8.66 (1H, dd, $J_{HP(trans\ S)}$ = 11.7 Hz, $J_{HP(trans\ C)}$ = 6.4 Hz, J_{HPt} = 19 Hz, H6), 7.86 (4H, ddd, $J_{HP(trans\ C)}$ = 11.7 Hz, $^3J_{HH}$ = 7.8 Hz, $^4J_{HH}$ = 1.4 Hz, *o*-H Ph *trans* C), 7.63–7.60 (3H, m, 2 *p*-H Ph and H7), 7.66–7.51 (6H, m, 2 *p*-H and 4 *m*-H Ph), 7.47–7.43 (5H, m, 4 *o*-H Ph *trans* S and H10), 7.40–7.36 (4H, m, *m*-H Ph), 7.27-7.23 (2H, m, H8 and H9), 4.89 (2H, m, Cp), 4.74 (2H, m, Cp), 4.32 (2H, br s, Cp*), 3.71 (2H, m, Cp*), 3.56 (3H, s, N-Me). ^{31}P NMR (101.3 MHz; CD_2Cl_2): 21.9 (d, J_{PP} = 22 Hz, J_{PPt} = 3096 Hz, P *trans* to S), 14.7 (d, J_{PPt} = 2262 Hz, P *trans* to C). IR (KBr disc): 3052 (w), 1670 (w), 1482 (w), 1436 (s), 1166 (m), 1098 (s), 1059 (br, s), 762 (m), 754 (m), 696 (s), 552 (m), 515 (m), 497 (m), 469 (m) cm^{-1}.

X-ray Structure Determinations. Crystals of **17** and **18**, suitable for X-ray analysis, were obtained by recrystallization from acetone/EtOAc and CH_2Cl_2/Et_2O/pentane, respectively. Experimental data (Table 5) for both compounds were collected at 150 K on a Delft Instruments FAST area detector equipped with a rotating anode FR591 generator (50 kV, 55 mA), a bufferboard and DEP image intensifier with Mo Kα radiation (λ = 0.710 69 Å, graphite monochromator), and an Oxford Cryostream low-temperature cooling system, controlled by a microVax 3200 and driven by MADNES software.[32]

The orientation matrix and unit cell parameters were determined with the ENDEX routine using 50 reflections with Bragg angles $\theta_{min} < \theta < \theta_{max}$ (Table 5) from two FIND 5-deg rotation ranges separated by 90° around the ω axis and subsequently refined during data processing using 250 reflections from each processed batch of data.

Data evaluation was performed off-line on a Vax station 4000/60 clustered with the diffractometer driving computer with frames transfer and processing taking place simultaneously with data collection, processing time not exceeding exposure time.

Slightly more than a hemisphere of data was collected for each compound (a 195-deg ω rotation around an arbitrary axis at χ = 0° plus two complementary "cusps" of 70°, each differing by 90° in φ at χ = 90°), with crystal-to-detector distance, detector swing angle, and other parameters chosen according to the diffracting properties of each crystal. Most notably, the fact that crystal **18** had a high mosaicity required that the between-frames increment and PAD parameter had to be increased so that the half-width of the peak would fit into five frames around the peak center (Table 5). The data was corrected for Lorentz and polarization effects and also for absorption using the program DIFABS.[33]

Both structures were solved by direct methods using the program SHELXS-86[34] and refined by full-matrix least-squares on F_o^2 using the program SHELXL-93.[35] In **17**, the phenyl rings were refined as idealized hexagons (C–C = 1.39 Å), with the ring hydrogens riding on their parents (C–H = 0.93 Å) and the methyl groups allowed to rotate about the C–C axis as regular tetrahedra (C–H = 0.96 Å). All non-hydrogen atoms were refined anisotropically, while the hydrogen atoms were assigned U(iso)'s equal to 1.2 times the U(eq)'s of the parent carbons. The BF_4^- anion showed some disorder, but refined successfully with one F atom split between two neighboring positions with partial occupancies 0.6667 and 0.3333. The final ωR_2 and the conventional R_1 values (Table 5) based on the refinement using 439 parameters and all 5132 unique data (excluding five reflections considered "bad" due to nonsystematic errors such as the reflection being obscured by the beam stop) were 0.080 and 0.032, respectively.

(32) Pflugrath, J. W.; Messerschmidt, A. *MADNES*, version 11 September, 1989; Delft Instruments: Delft, The Netherlands, 1989.

(33) Walker, N. P. C.; Stuart, D. *Acta Crystallogr.* **1983**, *A39*, 158. Adapted for FAST geometry by Karaulov, A., University of Wales College of Cardiff, 1991.

(34) Sheldick, G. M. *Acta Crystallogr.* **1990**, *A46*, 467.

(35) Sheldick, G. M. Manuscript in preparation.

Table 5. Crystallographic Data for **17** and **18**

	17	**18**
formula	$C_{42}H_{36}BF_4FeNP_2PtS$	$C_{76}H_{64}BF_4Fe_2NP_4Pt_2S$
molecular weight	986.47	1735.91
data collection T (K)	150(2)	150(2)
wavelength (Å)	0.71069	0.71069
crystal system	triclinic	hexagonal
space group	$P\bar{1}$ (No. 2)	$P6_3$ (No. 173)
a (Å)	9.666(2)	27.520(7)
b (Å)	11.645(3)	27.520(7)
c (Å)	17.894(4)	18.008(8)
α (deg)	72.860(10)	90.000
β (deg)	87.410(12)	90.000
γ (deg)	78.466(13)	120.000
V (Å^3)	1885.6(7)	11812(8)
Z	2	6
ρ_{calcd} (mg/m^3)	1.737	1.464
absorption coefficient (mm^{-1})	4.28	4.09
$F(000)$	972	5112
crystal size (mm)	0.20 × 0.15 × 0.05	0.50 × 0.20 × 0.20
detector-to-crystal distance (mm)	50.0	60.0
detector-to-beam angle (deg)	20.0	20.0
crystal mosaicity ϵ (deg)	0.88	1.81
exposure time per frame (s)	15	15
between frame increment (deg)	0.20	0.35
minimum and maximum absorption correction factors	0.988, 1.105	1.111, 1.436
θ range for data collection (deg)	2.15–24.93	1.68–22.39
index ranges	$-10 \le h \le 8$ $-13 \le k \le 13$ $-15 \le l \le 20$	$-28 \le h \le 17$ $-20 \le k \le 27$ $-12 \le l \le 18$
reflections collected	5946	19311
independent reflections	5137 (R(int) = 0.0365)	4639 (R(int) = 0.0795)
refinement method	full-matrix least-squares on F^2	full-matrix least-squares on F^2
data/restraints/parameters	5132/0/439	4634/388/591
goodness-of-fit on F^2	0.347	0.416
final R indices [$I > 2\sigma(I)$][a]	R_1 = 0.0277, ωR_2 = 0.0716	R_1 = 0.0353, ωR_2 = 0.0838
R indices (all data)	R_1 = 0.0322, ωR_2 = 0.0802	R_1 = 0.0434, ωR_2 = 0.1450
absolute structure parameter		0
largest diff peak and hole e·Å^{-3}	1.086 and –0.750	0.728 and –0.455

[a] $R_1 = \sum||F_o| - |F_c||/\sum|F_o|$ and $\omega R_2 = \{\sum[\omega(F_o^2 - F_c^2)^2]/\sum[\omega(F_o^2)^2]\}^{1/2}$.

The refinement of the structure of **18** was initially attempted with SHELX-76, but it did not proceed smoothly; some anisotropic displacement parameters became non-positive definite, and the R_1 factor remained above 0.07. When SHELXL-93[40] was used, its new features of restraining displacement parameters, SIMU, DELU, and EADP, considerably improved the structure; the R_1 value dropped to 0.0425, and all thermal ellipsoids were definite positive. At the same time, the Flack absolute structure parameter calculated by this program was 0.45(1), which indicated that the structure was a possible racemic twin. This was dealt with by applying the racemic twin matrix, TWIN –1 0 0 0 –1 0 0 0 –1 2, and refining a BASF scale factor; with the final BASF value of 0.4993, it is clearly an ideal example of racemic twinning. The final ωR_2 and R_1 values for 591 parameters and all 4634 data (omitting five "bad" intensities) were 0.0890 and 0.0434, respectively; the corresponding values for the 3793 reflections with $I > 2\sigma(I)$ were 0.0838 and 0.0353, respectively. The phenyl and cyclopentadienyl rings were idealized with the C–C bonds constrained at 1.39 and 1.42 Å, respectively. The hydrogen atoms were ignored. The BF_4^- anion was disordered and smeared over a large region; however, only one geometric position for this group was identified from the difference map, and this was refined with full occupancies for the five atoms and the B–F and F···F distances restrained at 1.40(5) and 2.30(5) Å, respectively. Finally, it should be noted that the treatment of the crystal of **18** as a racemic twin is entirely consistent with the unusually high mosaicity of the crystal and related difficulties in the data collection; it also provides an excellent example of the ability of SHELXL-93[40] to handle data from a less than perfect crystal.

In both refinements the weighting scheme used was $\omega = 1/\sigma^2(F_o^2)$ and the atom scattering factors were as in SHELXL-93.[40] Calculations were preformed on IBM PC 486 and DEC ALPHA AXP400 computers.

Synthesis of 19. 2,3-Dimethylbenzothiazolium BF_4^- (10 mg, 0.04 mmol) was added to a solution of 1,1′-bis(diphenylphosphino)ferrocene-η^2-etheneplatinum (**10**) (31 mg, 0.04 mmol) in CH_2Cl_2 (2 mL) and vigorously stirred for 30 min. After filtration, the yellow solution was transferred via cannula into light petroleum (50 mL) to precipitate the product as a pale yellow solid (39 mg, 98%). Mp dec > 178 °C. Anal. Calcd for $C_{43}H_{38}BF_4FeNP_2PtS$: C, 51.62; H, 3.83; N, 1.40; S, 3.20. Found: C, 51.32; H, 3.88; N, 1.56; S, 3.14. ^{1}H NMR (500 MHz; CD_2Cl_2): 7.86 (2H, dd, $J_{HP(trans\ C)}$ = 11.2 Hz, $^3J_{HH}$ = 8.1 Hz, *o*-H Ph *trans* C), 7.73 (2H, dd, J_{HP} = 11.8 Hz, $^3J_{HH}$ = 8.1 Hz, *o*-H Ph), 7.67 (1H, td, $^3J_{HH}$ = 7.5 Hz, $^4J_{HH}$ = 1.7 *p*-H Ph), 7.61 (1H, td, $^3J_{HH}$ = 7.4 Hz, $^4J_{HH}$ = 1.7 *p*-H Ph), 7.58–7.41 (11H, m, Ar), 7.34–7.26 (5H, m, 4 Ph and H10), 7.14 (2H, td, $^3J_{HH}$ = 7.8 Hz, $^4J_{HH}$ = 2.5, Ph), 5.06 (1H, m, Cp), 4.83 (1H, br s, Cp), 4.59 (1H, s, Cp), 4.53 (1H, br s, Cp), 4.30 (1H, br s, Cp), 4.25 (1H, s, Cp), 3.79 (1H, s, Cp), 3.45 (1H, br s, Cp), 3.40 (3H, s, N-Me), 2.14 (3H, d, J_{HP} = 3.2 Hz, J_{HPt} = 23.4 Hz, C-Me). ^{31}P NMR (101.3 MHz; CH_2Cl_2): 18.4 (d, J_{PP} = 20 Hz, J_{PPt} = 3298 Hz, P *trans* to S), 11.1 (d, J_{PPt} = 2212 Hz, P *trans* to C). IR (KBr disc): 3055 (w), 1482 (w), 1437 (m), 1168 (m), 1098 (s), 1056 (br, s), 752 (m), 697 (s), 554 (m), 517 (m), 492 (m), 472 (m) cm^{-1}.

Synthesis of 20 and 21. 2-Chloro-3-methylbenzothiazolium BF_4^- (11 mg, 0.04 mmol) was added to a solution of 1,1′-bis(diphenylphosphino)-ferrocene-η^2-etheneplatinum (**10**) (31 mg, 0.04 mmol) in CH_2Cl_2 (2.5 mL) in an 8-mm NMR tube and the suspension vigorously agitated. The immediate formation of the ring-expanded product **20** as the major component was observed by NMR. ^{1}H NMR (250 MHz; CD_2Cl_2): 7.98–7.11 (24H, m, Ar), 5.09 (1H, s, Cp), 4.81 (1H, s, Cp), 4.60 (2H, s, Cp), 4.33 (1H, s, Cp), 4.28 (1H, s, Cp), 3.86 (1H, s, Cp), 3.60 (3H, s, NMe), 3.48 (1H, s, Cp). ^{31}P NMR (101.3 MHz; CH_2Cl_2): 19.4 (d, J_{PP} = 19 Hz, J_{PPt} = 3222 Hz, P *trans* to S), 10.7 (d, J_{PPt} = 2542 Hz, P *trans* to C). Over a period of 90 h, this rearranged to **21**. The yellow solution was transferred via cannula into light petroleum (40 mL) to precipitate a pale yellow solid (38 mg). This contained dichloro(1,1′-bis(diphenylphosphino)ferrocene)platinum (6%), which was removed by repeated fractional recrystallization from MeOH. Mp dec > 188 °C. Anal. Calcd for $C_{42}H_{35}BClF_4FeNP_2PtS$: C, 49.41; H, 3.46; N, 1.37. Found: C, 49.12; H, 3.46; N, 1.22. ^{1}H NMR (250 MHz; CD_2Cl_2): 7.98 (4H, dd, J_{HP} = 10.6 Hz, J_{HH} = 7.3 Hz, Ph), 7.75–7.43 (13H, m, Ar), 7.33–7.25 (4H, m, Ph), 7.17 (1H, t, J_{HH} = 7.3 Hz, Ar), 7.04–6.98 (2H, m, Ar),

5.09 (1H, br s, Cp), 4.81 (1H, s, Cp), 4.74 (1H, s, Cp), 4.67 (1H, s, Cp) 4.34 (2H, s, Cp), 4.11 (3H, s, N-Me), 3.78 (1H, s, Cp), 3.68 (1H, s, Cp). ^{31}P NMR (101.3 MHz; CH_2Cl_2): 14.4 (d, J_{PP} = 16 Hz, J_{PPt} = 2390 Hz, P *trans* to C), 11.9 (d, J_{PPt} = 3683 Hz, P *trans* to Cl). IR (KBr disc): 3055 (w), 1674 (w), 1482 (w), 1437 (s), 1387 (w), 1169 (m), 1098 (s), 1056 (br s), 750 (s), 697 (s), 559 (m), 517 (m), 495 (s), 470 (m) cm^{-1}.

Synthesis of 22. 1,1′-Bis(diphenylphosphino)ferrocene-η^2-ethene-platinum (**10**) (31.1 mg, 0.04 mmol) and *S*,*N*,*N*-trimethylthioformamidinium BF_4^- (7.6 mg, 0.04 mmol) were dissolved in THF (2.5 mL) and then stirred for 1 h. The yellow solution was transferred via cannula into light petroleum (40 mL) to precipitate the product as a yellow solid (44 mg, 94%). Mp dec > 163 °C. Anal. Calcd for $C_{38}H_{38}BF_4FeNP_2PtS$: C, 48.53; H, 4.07; N, 1.49. Found: C, 48.47; H, 3.90; N, 1.28. ^{1}H NMR (500 MHz; $CDCl_3$): 9.96 (1H, dd, J_{HP} = 6.0 Hz, J_{HP} = 4.1 Hz, J_{HPt} = 20.1 Hz, PtC*H*=N), 8.08 (2H, m, Ph), 7.77–7.26 (18H, m, Ph), 4.98 (1H, s, Cp), 4.76 (1H, s, Cp), 4.66 (1H, s, Cp), 4.56 (1H, s, Cp), 4.23 (1H, s, Cp), 4.20 (1H, s, Cp), 3.63 (1H, s, Cp), 3.60 (3H, s, N-Me(*Z*)), 3.56 (1H, s, Cp), 2.97 (3H, s, N-Me(*E*)), 2.07 (3H, d, J_{HP} = 5.5 Hz, J_{HPt} = 50.2 Hz, S-Me). ^{31}P NMR (101.3 MHz; THF): 16.1 (d, J_{PP} = 23 Hz, J_{PPt} = 2779 Hz, P *trans* to S), 15.6 (d, J_{PPt} = 2186 Hz, P *trans* to C). IR (KBr disc): 3051 (w), 1619 (m), 1482 (w), 1436 (m), 1098 (s), 1084 (s), 1038 (s, br), 751 (m), 698 (s), 553 (m), 518 (m), 494 (m), 470 (m) cm^{-1}.

Acknowledgment. We thank SERC for a CASE studentship (to V.C.M.S.) in association with BP Research and for a grant toward the cost of the diffractometer. Johnson–Matthey kindly provided a loan of precious metal salts.

Supplementary Material Available: Extended version of Table 1, tabulation of electrospray MS data. X-ray structure files for compounds **17** and **18**, including atomic coordinates and equivalent isotropic displacements, bond lengths and angles, and anisotropic displacement parameters, hydrogen coordinates and isotropic displacement parameters for structure **17** (13 pages); tables of observed and calculated structure factors for **17** and **18** (23 pages). This material is contained in many libraries on microfiche, immediately follows this article in the microfilm version of the journal, and can be ordered from the ACS; see any current masthead page for ordering information.